POLITECNICO DI TORINO
Repository ISTITUZIONALE

Characterizing urban drainage networks through scaling laws and centrality metrics: Insights from the Turin case

Original
Characterizing urban drainage networks through scaling laws and centrality metrics: Insights from the Turin case / Eberrini, A., Ridolfi, L., Fellini, S.. - In: JOURNAL OF HYDROLOGY. REGIONAL STUDIES. - ISSN 2214-5818. - ELETTRONICO. - 65:(2026). [10.1016/j.ejrh.2026.103442]

Availability:
This version is available at: 11583/3018152 since: 2026-11-19T10:16:43Z

Publisher:
Elsevier

Published
DOI:10.1016/j.ejrh.2026.103442

Terms of use:

This article is made available under terms and conditions as specified in the corresponding bibliographic description in the repository

Publisher copyright

(Article begins on next page)

27 November 2026

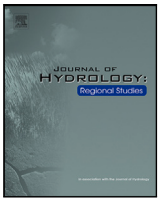
Journal of Hydrology: Regional Studies 65 (2026) 103442



Contents lists available at ScienceDirect

Journal of Hydrology: Regional Studies

journal homepage: www.elsevier.com/locate/ejrh





Characterizing urban drainage networks through scaling laws and centrality metrics: Insights from the Turin case

Anna Eberrini *, Luca Ridolfi, Sofia Fellini

Politecnico di Torino, Torino, Italy

ARTICLE INFO

Dataset link: https://doi.org/10.5281/zenodo.17702204

Keywords:
Urban drainage networks
Scaling laws
Complex network analysis
Urban hydrological response
Peak flow dynamics

ABSTRACT

Study Region: The study investigates the urban drainage system of Turin, a historically stratified city of about one million inhabitants.

Study Focus: Urban drainage networks (UDNs) are key components for stormwater management and flood risk mitigation. Understanding their structural characteristics, both topological and hydraulic, is essential to improve their hydrological response. This study investigates Turin's UDN through two complementary approaches: (i) identification of scaling laws, inspired by river-basin geomorphology; and (ii) application of weighted and unweighted centrality measures (Betweenness and Closeness) from complex network theory. Results are interpreted through a historical lens, dividing the network into four urban development phases, and a hydraulic lens, assessing the response to two rainfall events.

New Hydrological Insights for the Region: Three scaling laws were identified: Hack's law ($L \propto A^h$), the scaling between maximum discharge and drained area ($Q \propto A^c$), and the relationship between cross-sectional area and drained area ($S \propto A^p$). Historical development influences the scaling exponents, while longer rainfall events increase c, suggesting links with storage capacity. Betweenness centrality is primarily controlled by topology, whereas closeness is strongly affected by weighting. A significant correlation between closeness (C) and maximum flow (Q) suggests potential predictive capability. These results highlight the benefit of combining geomorphological and complex network tools for analysing real UDNs, providing a framework applicable to other urban contexts.

1. Introduction

Urban drainage networks (UDNs) are essential systems that manage stormwater runoff and mitigate flood risks. Their efficiency is increasingly challenged by growing urbanization and more frequent extreme weather events, linked to climate change (Ji et al., 2025; Kourtis and Tsihrintzis, 2021; Li et al., 2024; Miller and Hutchins, 2017; Yazdanfar and Sharma, 2015; Zhou, 2014). In this context, understanding the structural characteristics of UDNs, from both a topological and a hydraulic perspective, plays a key role in improving system performance and resilience. To this end, different approaches can be pursued, each of which makes a specific contribution to the interpretation of the system.

A useful perspective for understanding UDNs comes from comparing them with natural drainage networks, which provide an efficient model for water conveyance. However, although both develop with a tree-like structure, the two network types present significant differences from a topological, geometric and hydraulic point of view. These differences derive from the distinct processes that guide their formation. River networks are the result of natural processes of erosion and optimization of runoff along minimum

* Corresponding author.
E-mail address: anna.eberrini@polito.it (A. Eberrini).

https://doi.org/10.1016/j.ejrh.2026.103442
Received 30 January 2026; Received in revised form 18 March 2026; Accepted 8 April 2026
Available online 12 May 2026
2214-5818/© 2026 The Authors. Published by Elsevier B.V. This is an open access article under the CC BY license (http://creativecommons.org/licenses/by/4.0/).

slope paths; UDNs are designed and built to respond to specific urban and functional constraints, which lead them to be more articulated also in their structure.

A key analytical approach to systematically investigate these differences is the study of scaling relationships. Scaling laws are a quantitative reflection of the organization of a system, independently from its specific formation. In the case of river networks, the existence of these relations plays a key role and is well-documented in the literature (Hack, 1957; Horton, 1945; Rigon et al., 1996; Rodriguez-Iturbe et al., 1994; Rodriguez-Iturbe and Rinaldo, 1997; Tarboton et al., 1991). On the other hand, the application of these laws to UDNs is significantly less common. Yang et al. (2017) investigated the scaling and topology of the UDNs of two cities of very different sizes, analysing their evolution over decades through Hack's law and the exceedance probability distribution of upstream contributing area. Additionally, Achour et al. (2023) applied scaling laws to the combined sewer system of Paris, employing Horton–Strahler ordering and the exceedance probability of the drained area to characterize the network's structure.

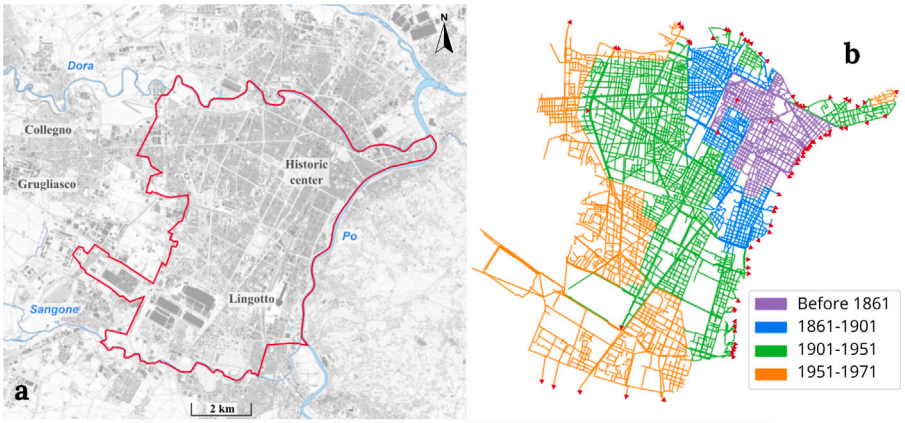
Another useful approach to study and understand the networks' structure involves the use of topological analysis tools derived from Complex Network Theory (CNT). CNT has found wide application across diverse fields, ranging from social and communication networks to real-world systems and Earth sciences (Estrada, 2012; Fellini et al., 2021; Newman, 2018; Phillips et al., 2015). In hydrology and water resources management, CNT has been successfully applied to a variety of systems and processes. It has been used to investigate the structure and optimality of river networks (Rinaldo et al., 2006), to analyse pressure dynamics and vulnerability in water distribution systems (Marsili et al., 2023; Simone et al., 2018; Vesipa et al., 2026), to study global virtual water trade (Suweis et al., 2011), and to explore the spatial dynamics of precipitation (Scarsoglio et al., 2013). In this context, UDNs can be considered as oriented graphs in which the nodes represent manholes, reservoirs and outflow points, while the edges correspond to the conduits, with the direction of each link indicating the direction of water drainage. These are spatial networks (Barthélemy, 2011), where nodes are located in three-dimensional physical space. Furthermore, assigning weights to the network links allows incorporating not only topological, but also quantitative information, relevant for the hydraulic operation of the system.

Recently, some studies have been carried out exploring the use of complex network analysis in natural and urban drainage systems, although such applications are still underdeveloped. For natural drainage basins, Sarker et al. (2019) investigated potential relationships between network vulnerability and centrality measures. Critical nodes, whose removal causes the greatest fragmentation of the river network, are compared with those ranked high in betweenness centrality. Another study examined the Tarin river basin in China, assessing eigenvector and betweenness centrality of nodes (Yu et al., 2024). The results show that highly central nodes were concentrated near mainstreams and source-mainstream intersections, emphasizing a correlation between centrality and system connectivity. Research focusing on UDNs' application is even more limited. Krueger et al. (2017) conducted a topological analysis of both the water distribution network and the sanitary sewer network of a large Asian city, exploring their spatial and temporal evolution through metrics such as network density, clustering coefficient, and node-degree distribution. Giustolisi et al. (2020) demonstrated the crucial role of node relevance in determining an accurate ranking based on specific centrality measures such as closeness and betweenness, using examples from social and infrastructural network. More recently, Simone et al. (2022) evaluated the use of both standard and newly introduced tailored complex network analysis metrics for vulnerability assessment and contaminant spread analysis. These tailored metrics were specifically developed within the study to incorporate intrinsic information about the system. Applied to a small synthetic network, the analysis showed that standard centrality measures (degree, harmonic, and betweenness) were insufficient to capture network behaviour, whereas the tailored metrics provided meaningful insights for assessing vulnerability and planning monitoring strategies.

Despite these contributions, important gaps remain in the current understanding of urban drainage networks. First, while scaling laws have been extensively investigated in natural river systems (Hack, 1957; Horton, 1945; Rodriguez-Iturbe and Rinaldo, 1997) and occasionally explored in UDNs (Yang et al., 2017), their interpretation and applicability to engineered systems are still not fully understood. Previous studies have mostly focused on geometric relationships, overlooking the potential to incorporate hydraulic quantities such as discharge or conduit cross-section. As a result, the connection between the morphological organization of UDNs and their hydraulic functioning under different rainfall conditions remains largely unexplored. Second, although CNT has recently been introduced as a promising framework for exploring UDN structure, most applications have relied on simplified or synthetic models. The potential of centrality-based metrics to capture the functional and hydraulic relevance of nodes within real drainage systems remains largely unexplored. In particular, the use of weighted centralities that explicitly incorporate hydraulic attributes (such as conduit length and discharge) has received little attention, despite its promise for linking network topology with the dynamic hydraulic response of the system.

To address these gaps, this work explores the capability of scaling analysis and complex network-based metrics to extract information about the topology and hydraulic behaviour of UDNs. It will be shown that, on one hand, scaling laws can be identified in UDNs and compared to those observed in river networks; on the other hand, centrality-based metrics can reveal meaningful topological patterns, helping to characterize the functional role of nodes within the urban hydraulic system. In this context, centralities offer valuable insights into network organization and can support planning and maintenance strategies. The analysis is carried out from two different points of view: the first, of a historical nature, considers the influence of urban development on the network; the second, of a hydraulic nature, analyses the network's response to two rainfall events of different durations and their effects on the weighted centralities.

To this aim, the focus is on a portion of the drainage network of the city of Turin, a metropolitan area with 886,837 inhabitants and a total surface of 130 km^2. Turin's drainage system is increasingly vulnerable due to high soil sealing (Biasin et al., 2023) and a reliance on a natural hydrographic network that is often overwhelmed by surface runoff (Salata et al., 2021). As analysed by Cremonini et al. (2024), intense convective rainfall frequently exceeds the sewage capacity, causing rapid flash floods and highlighting the need for advanced early warning systems and sustainable mitigation strategies like nature-based solutions (Biasin



	Before 1861	*1861-1901*	*1901-1951*	*1951-1971*	Entire network
Nodes	4115	4048	9436	5814	23413
Links	4466	4416	10261	6038	25181

Fig. 1. (a) Study area; (b) Partitioning of the UDN according to the different periods of urban development in the city of Turin, the red triangles indicate the network's outfalls. The table shows the number of nodes and links in both the partitioned and the entire network.

et al., 2023). The UDN interacts with the natural hydrographic network, which includes the River Po and its tributaries, making it important to understand flow transport and network behaviour for flood mitigation and urban water management. It is a separate UDN, whose system dedicated to the management of rainwater will be analysed. The Turin network presents a multi-level complexity, due to the fact that the city and the network have evolved and transformed in parallel over the last 150 years. The choice of this case study is also motivated by the availability of a large dataset and a detailed hydraulic study on the network, recently requested by local water utility (Ridolfi et al., 2023).

The article develops through the following sections: Section 2 describes the study area and presents the methodological framework adopted; Section 3 discusses the results of both analyses, highlighting the effects of historical stratification and the differences observed between the two rainfall events. Finally, Section 4 concludes the work with a summary of the main findings and final considerations.

2. Materials and methods

This section describes the study area and the hydraulic simulations used to model the behaviour of the UDN, and presents the methods applied for the analysis of the network, including the scaling laws and centrality metrics considered.

2.1. Study area

Turin is a metropolitan city located in the north-west of Italy and is the fourth largest city in the country by population. The water services of Turin are managed by Metropolitan Water Company of Turin (Società Metropolitana Acque Torino, SMAT), which plans, manages and administers the urban integrated water cycle. The network separates the management of rainwater and wastewater and the part dedicated to the management of rainwater was examined.

A detailed hydraulic modelling of the network was carried out by Ridolfi et al. (2023) to study its functioning and identify possible critical points. The reason for the study is related to some criticalities presented by the network during intense meteoric events. The UDN of the city was initially divided into 33 basins, grouped into four hydraulically independent areas. The largest of these areas, shown in Fig. 1, was considered in this work. The corresponding modelled network has 23,413 nodes, corresponding mainly to manholes, and 25,181 links. This implies that multiple nodes often lie along the same pipeline. Over the entire network, conduit lengths exhibit a mean value of 31.1 m with a standard deviation of 28.2 m. The cross-sectional area of the conduits has an average value of 0.72 m^2 with a standard deviation of 0.66 m^2. The UDN covers the oldest part of the city's historic centre as well as recently urbanized areas, such as the Lingotto district (Fig. 1a). The area includes all drainage basins bounded to the north by the Dora river, to the west by the municipalities of Collegno and Grugliasco, to the south by the Sangone stream, and to the east by the Po river. The total area drained by the network is 44,136 km^2, and is populated by approximately 650,000 inhabitants (14,727 inhabitants per km^2 on average across the entire study area).

To investigate how the layered urban development has influenced water management, the network was examined in connection with the city's historical growth. Starting from the urban maps of Turin (Falco and Morbelli, 1976), four main historical periods of urban development have been identified, each of which has been associated with the corresponding part of the UDN (see Fig. 1b). The pre-1861 area corresponds to the historic centre, while subsequent developments (1861–1901, 1901–1951, 1951–1971) expanded concentrically towards the south-west. The 1901–1951 area has the most extensive network in numerical terms, with

approximately twice as many manholes and pipes as the others (see table in Fig. 1). Although urban development continued after 1971, most of the infrastructure can be assumed to have been developed during these periods. The present analysis is therefore based on the current network configuration provided by the water utility (SMAT), while the historical subdivision is used as a proxy to relate the structural characteristics of today's UDN to the major phases of urban expansion that originally shaped its development.

2.3. Hydraulic simulations

As mentioned in the previous section, the hydraulic model and related simulations were developed in a previous collaboration with SMAT, the company managing the city's water utilities (Ridolfi et al., 2023). All data and results reported in this subsection refer to that work. Topological and hydraulic data, including pipe sections, lengths, roughness and altimetrical quotes, required for hydraulic simulation, were provided by SMAT. Processing and numerical simulations were carried out with the EPA SWMM software, for modelling stormwater runoff and the behaviour of the UDN. The study area was divided into 33 basins—chosen so that each was as hydraulically homogeneous as possible—and each basin was further subdivided into many sub-basins (approximately 30–50, depending on their characteristics) in order to represent the intra-basin variability in land use, soil infiltration capacity, roughness, and slope. Each sub-basin was associated with the nearest manhole, so that in the simulation the water drains through that manhole. Infiltration and runoff were modelled based on the land use and soil properties of the sub-basins, adopting the typical parameter values indicated by EPA guidelines (Rossman and Simon, 2022). A detailed analysis on the hydraulic parameters (perturbed one at a time) confirmed the robustness of the values adopted in this study, including infiltration parameters, surface roughness, depression storage, and sub-basin residence times. Both Horton and Curve Number methods were tested to simulate soil infiltration.

To identify possible critical points in the UDN from a hydraulic perspective, the response of the network was simulated under two rainfall events. Both events had a return time of 5 years and were characterized by spatially uniform intensity, statistically described using Gumbel's probabilistic model. The choice of a five-year return period stems from the hydraulic simulation work commissioned by the water utility SMAT, which aimed to identify the hydraulically weak points of the network with a frequency of a few years. Therefore, not extremely rare devastating events, but rather critical events that had occurred repeatedly over the past 20–30 years; events that had caused problems for residents with a "fairly" frequent frequency. This choice is also consistent with the Italian regulatory framework (DPCM, 1996), which identifies a five-year return period as the reference threshold for the serviceability of urban drainage systems. The two selected event durations, lasting 10 min and 1 h, were taken from the *Heavy Rainfall Atlas of Piedmont* (ARPA Piemonte, 2013) published by the Regional Agency for Environmental Protection. These durations were chosen to represent two typical rainfall conditions: a short and intense event, and a longer one with more moderate intensity. The rainfall-duration-intensity curves do not show statistically significant spatial variations at the scale of the city of Turin; for this reason and to stress the entire drainage network simultaneously in a remarkable way, a uniform spatial distribution of precipitation was adopted. Unfortunately, flow measurements within the network are not available. However, the reliability of our modelling was positively tested by comparing the critical points (high-pressure pipelines, local floods, etc.) resulting from numerical simulations with the information held by the water utility in the form of network management experience (past interventions, emergencies, etc.). From the simulations of the hydraulic response of the model, the maximum discharge (Q_{max}) in each conduit in both scenarios was extracted, providing a quantitative basis for the subsequent analysis of network scaling and weighted centralities.

2.4. Scaling analysis

Understanding whether UDNs exhibit scaling laws can provide valuable insights into their structure. Scaling behaviours have been extensively observed in natural systems, particularly in river networks. The concept of Optimal Channel Networks represents river networks as systems that self-organize over time, shaped by environmental and geological conditions (Rodriguez-Iturbe and Rinaldo, 1997). This leads to a tendency towards self-similarity (Langhaar, 1962), which can be mathematically expressed through specific scaling laws. This study investigates whether similar properties emerge in the case of the Turin UDN. To this aim, three relationships are analysed: the first two are extensively documented in river network analyses; in addition, a third law is proposed in this study.

One of the fundamental scaling laws in river networks was introduced by Hack (1957) and relates the length L_{Hack} of the longest stream within the drainage region to the drained area A:

$$L_{Hack} \propto A^{h_1}. \tag{1}$$

The exponent h_1 for rivers has been shown to belong to a small range, $h_1 \in [0.5, 0.7]$ (Hack, 1957; Rigon et al., 1996; Sassolas-Serrayet et al., 2018).

The study by Yang et al. (2017) confirms the applicability of this law to UDNs, supporting the hypothesis that artificial drainage systems may exhibit scaling behaviours similar to natural river networks. However, unlike natural rivers, identifying the main course in a UDN is less straightforward, as engineered drainage systems often include multiple parallel branches and non-hierarchical flow patterns. In these systems, L_{Hack} can be defined as the maximum distance, in terms of the shortest path l, between a considered control point b and an apex point a within the UDN (see Fig. 2a). Control points b are selected to represent locations from which upstream paths are traced to determine scaling properties. In the present study, following the methodology commonly used in river basin analysis, control points include both confluence nodes (indicated by a green dot in Fig. 2a), where at least two conduits meet, and designated outfall nodes (shown as blue triangles in Fig. 2a). Formally, the law is expressed as: $L_{Hack} = \max_{a \in \mathrm{UDN}} l_{ba}$.

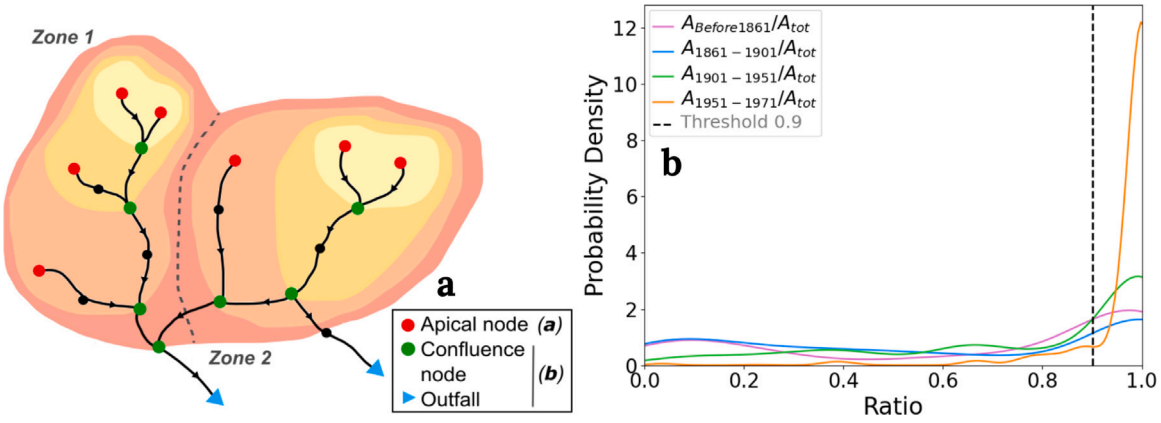


Fig. 2. (a) Schematic diagram of a water network in which the drained area belongs to two different historical zones, *zone 1* and *zone 2*, separated by the dashed line. The area drained by the various confluence points (green dots) gradually expands along the path towards the outfall (blue triangle), as indicated by the different colour gradations. (b) For each zone, the probability density that a control point belonging to the specific historical zone drains the area belonging to the same zone is reported. The dashed line marks the threshold: only control points with a probability greater than 90% are considered in this study.

This definition allows identifying an equivalent "main path" for each drainage area while accounting for the actual topology of the network.

To complement this representation and overcome the limitations associated with identifying a single dominant flow path, an alternative definition of length, L_{tot}, is introduced. This is defined as the total sum of the lengths of all pipes within the drained area. This formulation provides a more comprehensive measure of the network's spatial development and allows exploring whether scaling relationships persist when considering the entire drainage infrastructure rather than only the main flow path. The corresponding scaling law can be expressed as:

$$L_{tot} \propto A^{h_2}. \tag{2}$$

The second scaling law emerging in river networks links the discharge to the drained area (Rodriguez-Iturbe and Rinaldo, 1997):

$$Q \propto A^{c} \tag{3}$$

where the exponent c takes the value 0.75 for river networks, if the bankfull discharge is considered (Leopold et al., 2020). In drawing an analogy with UDN, here it is assumed that the bankfull discharge of a river can be compared with the maximum discharge Q_{max} passing through the UDN in the considered control section, providing a conceptual framework to analyse peak flows in the network.

Finally, the potential existence of a scaling relationship linking pipe cross-sectional geometry to the drained area is investigated, since conduit dimensions are designed to accommodate the expected runoff. Although hydraulic design imposes a positive relationship between drained area and conduit size, it remains unclear whether this follows a regular scaling behaviour, comparable to that observed in natural drainage systems. In rivers, cross-sectional geometry has been shown to scale with discharge (Leopold and Maddock, 1953), and discharge itself scales with the upstream contributing area, giving rise to well-defined geometric scaling laws. Testing this analogy in engineered systems allows us to assess whether urban drainage networks exhibit self-similar geometric organization, or whether design constraints and urban development introduce discontinuities. Using the available data on pipe shapes and sizes for the Turin UDN, the following possible scaling is explored:

$$S \propto A^{p} \tag{4}$$

where S is the local cross-sectional area of the conduit at the control point, while A denotes the upstream contributing (drained) area associated with that point. Since the scaling quantities are evaluated at network nodes, the local cross-section is referred to the conduits entering the node. The cross-sectional area of each pipe is derived from the available geometric information, using direct geometric formulas for regular sections and numerical integration for irregular profiles.

To apply scaling relations (1)–(4), the first essential step is to compute, for each control point, the quantities L_{Hack}, L_{tot}, Q_{max}, S and A. As one moves downstream towards the outfall, the area drained by the various control points gradually expands, as indicated by the different colour gradations in Fig. 2a. When scaling the UDN subdivisions based on historical development, it is important to account for their hydraulic interdependence: the drainage area of a given control point may extend across multiple historical sectors. In Fig. 2a, for example, a control point (green) belonging to historical zone 1 drains the entire darker-shaded area shown in the figure, which includes both zones 1 and 2, making it impossible to treat the two zones as hydraulically independent. To ensure that the control points used for scaling law analysis are representative of a single historical zone, a filtering criterion is applied: for each historical zone, only control points for which at least 90% of the drained area falls within the same zone are retained.

Fig. 2b shows the probability density functions of the ratio between the area drained within the same historical zone as the control point and the total drained area. For all four historical periods, this ratio exceeds 0.9 in a large number of cases, as indicated by the distribution peaks near 1 in Fig. 2b. The steep and narrow peak for the 1951–1971 period suggests that this zone is hydraulically more self-contained than the others. This reflects the emergence of newly urbanized areas with dedicated drainage infrastructure, less interconnected with older portions of the network. By applying the 90% threshold, the analysis minimizes cross-zone hydraulic influence and ensures that the derived scaling relationships primarily reflect the internal dynamics of each historical zone. A sensitivity analysis on the threshold confirms the robustness and consistency of this choice.

2.4.1. Statistical tests

To quantify the scaling shown by Eqs. (1)–(4), a linear regression is performed on the log-transformed variables for each relationship, with the resulting slope coefficient indicating the scaling exponent. The statistical significance of the regression is assessed using a t-test on the slope (Montgomery et al., 2021).

To test whether the regression slopes obtained for the same scaling law differ significantly across different historical zones, a multiple linear regression model is formulated, incorporating a dummy variable to distinguish between the two datasets and an interaction term with the continuous predictor (Montgomery et al., 2021). The significance of the slope difference is assessed via a t-test on the interaction coefficient.

2.5. Complex network-based centrality metrics

Complex network analysis applied to water systems models the pipe intersections as nodes and conduits as connecting edges. The flow direction defines the orientation of the links in the resulting directed network. Centrality analysis is a fundamental approach in network analysis, used to rank nodes according to their influence. However, the concept of centrality, originally developed in the sociological domain, must be adapted to spatial networks, where geometric constraints and physical implications cannot be neglected (Barthelemy, 2022; Crucitti et al., 2006; Fellini et al., 2020). The importance of a node depends on the network's structure, type, and topology; consequently, different centrality measures have been developed to capture these aspects (Giustolisi et al., 2020; Rodrigues, 2018). For example, nodes with the greatest number of connections are not always the most influential in the flow propagation processes, since their position, whether central or peripheral, can also have a significant impact (Kitsak et al., 2010).

This study focuses on two key metrics to assess their effectiveness in representing the importance of nodes: betweenness centrality and closeness centrality. Betweenness centrality measures how frequently a node lies on the shortest paths connecting other nodes in the network, thus identifying nodes that potentially play a key role in the transmission of flows through the system. Closeness centrality, instead, quantifies how close a node is to all the others in terms of shortest path distance, providing an indication of how rapidly a process can spread from that node across the network. Each metric is calculated both in unweighted form, to analyse the topological contribution alone, and in weighted form, where weights w are assigned to each link to include the geometric and hydraulic characteristics of the pipes. To this aim, the following link weights are considered: (i) the sum L of the lengths of each pipe between two connected nodes; (ii) the maximum discharge Q_{max} and its inverse Q_{max}^{-1} during the simulated rain events; (iii) the maximum discharge over the cross section Q_{max}/S and its inverse S/Q_{max} during the two rain events, which are indicative of the average velocity through the conduit and its inverse. To simplify the notation, the maximum discharge will hereinafter be denoted as Q^{10min} and Q^{1h}, referring to the 10-minute and 1-hour rainfall events, respectively.

Before applying the metrics, the network is simplified through a contraction process that preserves its topological and functional properties. In fact, since the network has a large size, it contains redundant elements that do not contribute significant information but increase computational complexity. In particular, intermediate nodes, where no bifurcations occur and that connect only two pipes, can be removed without altering the network's connectivity or flow dynamics, thus simplifying the overall representation. The preprocessing consists of the following operations: (i) *identification of intermediate nodes*, which are nodes with both in-degree and out-degree equal to 1, that do not add structural information; (ii) *edge contraction*, where these nodes are removed and their connecting paths replaced with a single direct edge linking the initial and final nodes; and (iii) *weight aggregation*, in which the new edge's weight is computed based on the type of metric: additive weights (e.g. length L) are summed, while averaged weights (e.g. maximum flow rate Q) are calculated as the mean of the original segment values. This process iterates until no further contractions are possible.

Table 1 provides an overview of the topological and hydraulic characteristics of the contracted network in the different historical periods. The number of nodes and links shows how the amount of data decreases compared to the original network (Fig. 1) after the contraction process. The subnetwork corresponding to the period *1901–1951* contains the highest number of nodes and edges.

The average length of the conduit L shows a constant increase over time, from 80.60 m (*Before 1861*) to 147.04 m (*1951–1971*), indicating a trend towards longer connections in the more peripheral areas of the city. The coefficient of variation (CV) remains low and stable throughout all periods, likely due to the regular grid structure of Turin's street network, except for the period *1951–1971*, when it peaks at 1.21, suggesting greater heterogeneity in the lengths of the conduits. As for the maximum discharges Q^{10min} and Q^{1h}, mean and CV indicate significant variability across historical periods. The highest CV values, for both rainfall events, occur in the period *1861-1901*, implying a more heterogeneous distribution of the discharge in that part of the network.

The mean cross-sectional area S shows a slight increase over time, while its CV decreases slightly, reflecting in general a standardization of the dimensions of the conduits independent of the historical period.

Table 1
Topological and hydraulic characteristics of the network after pre-processing, starting with the number of nodes and the number of links. Mean (μ) and coefficient of variation (CV) of the distribution of pipe lengths L, maximum flow rates Q, cross-section area S and drained area A are then reported for the different historical zones.

Zone	Nodes	Links	L [m]		$Q^{10\,min}$ [l/s]		$Q^{1\,h}$ [l/s]		S [m^2]		A [km^2]	
			μ	CV	μ	CV	μ	CV	μ	CV	μ	CV
Before 1861	1029	1374	80.60	0.89	1014.08	1.48	503.51	2.15	0.64	0.90	0.10	1.82
1861–1901	994	1380	87.65	0.88	1116.54	2.09	587.88	2.81	0.71	1.10	0.05	1.19
1901–1951	2226	2883	105.57	0.86	1418.954	1.78	936.94	2.29	0.72	0.86	0.17	1.90
1951–1971	1210	1446	147.04	1.21	1406.59	1.67	854.80	2.34	0.76	0.83	0.28	1.58

2.5.1. Betweenness centrality

Betweenness centrality (Freeman, 1977; Newman, 2018) quantifies the importance of a node based on the frequency with which it lies on shortest paths between pairs of nodes. For a node u in a directed network, the normalized betweenness centrality $B(u)$ is defined as

$$B(u) = \frac{1}{(n-1)(n-2)} \sum_{s,t \neq u} \frac{n_{st}(u)}{n_{st}}, \tag{5}$$

where $n_{st}(u)$ denotes the number of shortest paths between nodes s and t passing through u, and n_{st} is the total number of shortest paths between s and t, with s and t spanning the entire network. The factor $(n-1)(n-2)$ serves as a normalization for directed graphs of size n, where n denotes nodes of the considered network.

For weighted networks, the metric is extended by defining path length as the sum of edge weights (Brandes, 2001). Weighted betweenness centrality $B_w(u)$ is computed analogously, where $n_{st}^w(u)$ and n_{st}^w denote the counts of weighted shortest paths passing through u and the total weighted shortest paths between s and t, respectively.

In general, a node with high B plays a pivotal role in the flow of information between other nodes. While, without weights, centrality depends purely on the network topology, introducing weights constrains the choice of the shortest path: a preferred path will be the one that minimizes the sum of the weights along the path. For example, if the weight is inversely proportional to the maximum discharge (Q^{-1}), shorter paths will be chosen through pipes with a higher discharge, since a high discharge reduces the "cost" of the path. Conversely, if the flow rate is at the numerator of the weight, paths through lower-flow pipes are preferred.

2.5.2. Closeness centrality

According to the metric of closeness centrality, a node is more central in the network the closer it is to all other nodes. Since the network studied is not strongly connected, i.e. not all nodes are mutually reachable, it is not possible to directly calculate standard closeness centrality, as some distances between nodes are infinite. To address this, the metric is computed separately for each connected component and scaled by its size (Wasserman and Faust, 1994). In a directed graph with multiple connected components, the *closeness centrality (C)* of a node u is defined as:

$$C(u) = \frac{n_u - 1}{\sum_{v \neq u} d(v,u)}, \tag{6}$$

where $d(v,u)$ represents the shortest path incoming distance from node v to node u, where v spans the entire network; $n_u - 1$ denotes the number of nodes within the connected component of u, excluding u itself. For weighted graphs (Saxena and Iyengar, 2020), the weighted $C_w(u)$ is defined similarly, replacing the shortest path distance $d(u,v)$ with the weighted shortest path distance $d^w(u,v)$, that accounts for edge weights.

A node with a high C is efficiently connected to the rest of the network, meaning it can quickly reach other nodes. Conversely, a low value of C indicates that a node is more peripheral and requires more steps to reach other parts of the network. Without weights, proximity depends solely on the topological distance, i.e., the number of steps (pipes) between the nodes. Similarly to betweenness, introducing weights alters the definition of distance and the physical meaning of the metric. For instance, if the weight represents length L, closeness reflects physical proximity, whereas if it represents the inverse of discharge Q^{-1}, nodes connected through high-flow pipes appear closer, reflecting hydraulic efficiency (Fellini et al., 2020).

3. Results and discussion

3.1. Scaling properties of the Turin drainage network

The power laws introduced in Section 2.4 are investigated, considering both the historical-urban evolution of the network and the distinction in the hydraulic response to the two possible rain events. First, the existence of the scaling laws and their dependence on rainfall events are assessed (Section 3.1.1). Then, the evolution of the scaling coefficient over time is investigated, considering the different periods of network construction. (Section 3.1.2). Finally, the scalings are compared with those of natural river networks (Section 3.1.3).

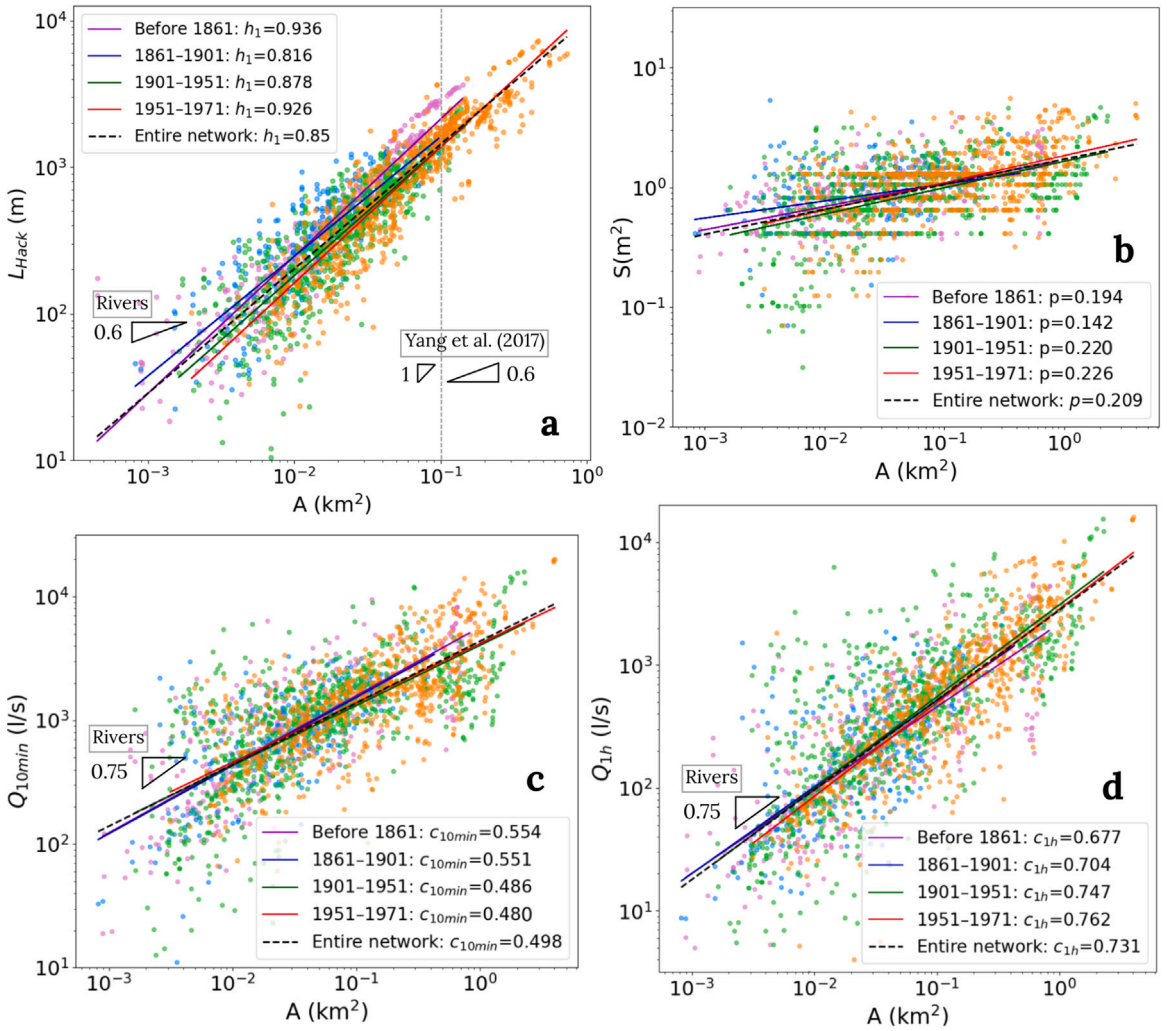


Fig. 3. Scaling relationships applied to the UDN of Turin. (a) Main channel length (L_{Hack}) versus drainage area (A); (b) pipe cross-section area (S) versus drainage area (A); (c) maximum discharge for the *10 min* rainfall event (Q^{10min}) versus drainage area (A); (d) maximum discharge for the *1 h* rainfall event (Q^{1h}) versus drainage area (A). The scatter plots are shown in log–log scale and fitted with linear regression. The black dashed line represents the regression line for the entire network, while the coloured lines correspond to the four partitions based on periods of urban development. The triangles represent the typical slopes for river basins and that one obtained by Yang et al. (2017) for $L_{Hack} \propto A^{h_1}$.

3.1.1. *Existence of scaling laws for UDNs*

Fig. 3 presents the scaling relationships between drained area and three key hydraulic and geometrical variables (see Eqs. (1)–(4)): channel length (panel a), cross-sectional area (panel b), and maximum discharge (panels c–d) for two rainfall durations (10 min and 1 h). All panels display a clear power-law trend, observed consistently across the entire drainage network and its historically defined subnetworks. This behaviour is further supported by the statistical results shown in Table 2, where the exponents of the power laws for the entire network and for the historical partitions are reported, along with the corresponding t-test results.

The existence of well-defined scaling laws suggests that the urban drainage network exhibits a hierarchical and self-similar structure, where geometric and functional properties repeat across different spatial scales. Relationships of this type are commonly observed in natural branched networks, such as river basins, where they emerge from the hierarchical organization of the drainage structure and the progressive aggregation of contributing areas (Rodriguez-Iturbe and Rinaldo, 1997). In these systems, power-law relationships reflect the geometric and hydraulic constraints that govern the development of efficient flow paths across multiple spatial scales. The observation of similar behaviour in urban drainage networks therefore suggests that, despite being engineered systems, they may inherit structural and organizational properties comparable to those of natural transport networks. From a practical standpoint, these relationships are particularly valuable because they allow for an *a priori* assessment of hydraulic characteristics (e.g., conduit size or expected discharge) based solely on the contributing area. This is especially relevant for the design or extension of networks in areas where only limited spatial or hydrological information is available.

Table 2
Table summarizing the exponents obtained for the power laws, in the entire network and in the four historical-urban partitions.

Power law	*Before 1861*	*1861–1901*	*1901–1951*	*1951–1971*	Total UDN	Rivers
$L_{hack} \propto A^{h_1}$	0.936***	0.816***	0.878***	0.926***	0.85***	0.6
$L_{tot} \propto A^{h_2}$	0.959***	0.917***	0.954***	0.961***	0.922***	0.6
$Q_{10\,\mathrm{min}} \propto A^{c_{10\mathrm{min}}}$	0.554***	0.551***	0.486***	0.480***	0.499***	0.75
$Q_{1\,\mathrm{h}} \propto A^{c_{1\,\mathrm{h}}}$	0.677***	0.704***	0.747***	0.762***	0.731***	0.75
$S \propto A^{p}$	0.194***	0.142***	0.220***	0.226***	0.209***	–

*** Next to the result indicates a positive result in the regression t-test, with a p-value $p_v \leq 0.01$.

For the scaling between length and drained area, the exponents h_1 and h_2—relating, respectively, the main channel length (L_{Hack}) and the total network length (L_{tot}) to the drained area—take on similar values close to 0.9 across all cases, with $h_1 < h_2$ consistently (see Table 2). This similarity suggests that the network retains a certain degree of topological coherence despite the different definitions of contributing length. For this reason, and for the sake of clarity and conciseness, the following analysis focuses on the Hack formulation, which is also the only length-based relationship reported in Fig. 3a.

From a geometric standpoint, one would expect an exponent of around 0.5 in the $L \propto A$ relationship, as in regular shapes (e.g., squares or circles) length typically scales with the square root of area. The significantly higher exponents observed here (close to 0.9) indicate more tortuous and articulated conduit paths than simple geometry would suggest. In this perspective, the exponent in the L–A scaling law acquires a hydraulic–geometric meaning: it reflects the tortuosity and spatial density of the network. In branched transport systems, higher exponents indicate that flow paths become progressively longer relative to the contributing area, revealing a more articulated and space-filling network organization. In urban drainage networks, this behaviour is consistent with construction constraints, where pipes must adapt to existing roads, buildings and infrastructure.

The h_1 exponents obtained in this study are comparable to those reported by Yang et al. (2017), who analysed three UDNs of different sizes. In their work, a power-law behaviour emerged regardless of basin size, showing two distinct segments in the log-transformed drained area space (see the two triangles at the dotted line in Fig. 3a): for small $\log(A)$, the slope was close to 1, while for larger areas it dropped to around 0.6. This behaviour supports the hydraulic–geometric interpretation described above: smaller basins typically correspond to dense urban cores, where longer and more intricate conduits are needed to efficiently drain the entire area. As basin size increases, it often includes main collectors that are straighter and designed to convey water rapidly away from urban zones.

The Turin UDN covers a total area of 44 km^2, with historical sub-areas on the order of tens of km^2. In terms of size, both the entire network and its partitions fall between the smallest case analysed by Yang et al. (2017) (Wahiawa, 7.2 km^2) and the intermediate case (Honouliuli, 85.1 km^2). Accordingly, no distinct break between two scaling regimes is observed in our results. Except for a few outliers at low $\log(A)$ values, the relationship follows a fairly consistent power-law trend, with h_1 values ranging from 0.8 to 0.9. This suggests that, despite differences in city structure, history, and size (i.e., Turin compared to Honouliuli and Wahiawa) the presence of this scaling behaviour remains robust.

Panels c and d in Fig. 3 confirm the existence of a scaling law between maximum discharge (Q) and drained area (A). The relationship is sublinear, with scaling exponents c ranging from approximately 0.5 (for the 10-minute event) to 0.7 (for the 1-hour event). This behaviour is in line with the hydrological response of the basins considered here. The response of a basin is in fact governed by its time of concentration, which defines the rainfall duration (uniformly distributed over the basin) for which the entire basin contributes to the peak discharge at the control section. When the rainfall duration is equal to or greater than the time of concentration, the whole basin contributes to the peak discharge (Butler et al., 2018); if the rainfall duration is shorter, only a portion of the basin contributes. In light of this, the exponents c_{10min} and c_{1h} being smaller than 1 indicate that the rainfall durations considered are not sufficient for all basins (including those with the largest areas) to fully contribute to the peak discharge. In fact, aside from local heterogeneities in land use across the basins (all of which are urban), if the entire drained area contributed fully to the maximum discharge, Q would scale proportionally with A, yielding an exponent $c = 1$. The hydraulic reason why larger basins contribute only partially to the peak discharge lies in their greater surface area and their larger temporary water storage capacity—such as infiltration into soils, runoff along streets, and filling of conduits—which increases their time of concentration. The higher value of the exponent c_{1h} compared with c_{10min} confirms this interpretation: as rainfall duration increases, it tends to approach the time of concentration of the larger basins, and therefore the exponent approaches 1. In other words, a larger portion of the basin area contributes to the peak discharge.

Turning to the link between pipe cross-section S and drainage area A (panel b in Fig. 3), it can be observed that the values of the cross-section tend to cluster on the standard sizes of the conduits used to build the drainage networks. Despite this discretization, the statistical test still shows the existence of a clear, statistically significant trend, with a value of p around 0.2. On average, therefore, the cross-section S increases with the drained area A, exhibiting a marked sublinear behaviour. Combining the scaling relationships $Q \propto A^c$ (with $c < 1$) and $S \propto A^p$, we obtain $S \propto (A^c)^{p/c} \propto Q^{p/c}$, a relationship between two local quantities. For the values estimated in this study, $p/c < 1$. This implies that the cross-sectional area grows (locally) more slowly than the flow rate. This result suggests the existence of a structural constrain of the drainage system: as the flow rate increases, the increase in the hydraulic capacity of the pipes is not proportional. This means that as conduits farther from the apical points of the network are considered (that is, moving towards the outlet), their capacity to convey the flow is not ensured only by increasing the cross-sections, but has to be

a

Period (1)	Period (2)	h_1	h_2	c_{10min}	c_{1h}	p
Before 1861	1861-1901	***	***			*
Before 1861	1901-1951	**		**	*	
Before 1861	1951-1971			***	***	
1861-1901	1901-1951	*	*			***
1861-1901	1951-1971	***	**	**		***
1901-1951	1951-1971	**				

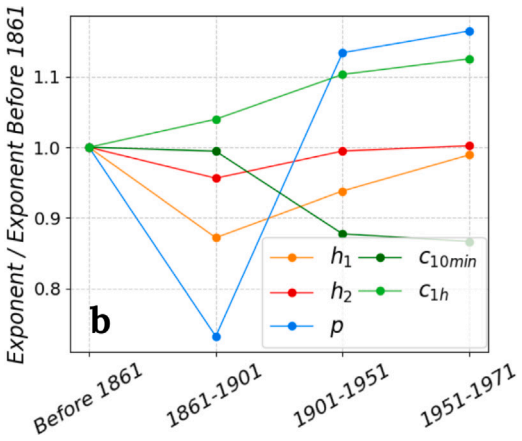


Fig. 4. The table on panel (a) presents the results of the statistical pairwise comparison tests on the regression lines across the four urban-historical partitions. All power-law exponents are compared. Asterisks denote significance levels: *** a p-value $p_v \leq 0.01$, ** indicates $0.01 < p_v \leq 0.05$ and * indicates $0.05 < p_v \leq 0.1$. Absence of asterisks indicates that no significant difference was found. In the plot on panel (b), scaling exponents are normalized to the values obtained in the *Before 1861* period for the power laws analysed. The historical periods are shown on the x-axis.

also achieved by appropriately increasing the flow velocity (e.g., by increasing the slopes of the conduits). If this is not possible, the consequence is an increase downstream in the risk of local critical conditions; for example, backflows or localized flooding. Finally, it is worth noting that the ratio p/c is approximately 0.42 and 0.29 for rainfall durations of 10 min and one hour, respectively. This means that the increase in criticality towards downstream sections is higher in the case of longer rainfall durations.

3.1.2. Impact of historical evolution

In order to better understand the evolution of the urban drainage network over time, the scaling laws for the historically delimited subnetworks are tested (Section 2.4.1). The table in Fig. 4 panel a summarizes the results of a two-by-two significance test performed on the scale exponents obtained for each period. In this test, each pair of periods is compared to assess whether their differences are statistically significant. The results show a temporal evolution in the structure of the network. A threshold of p-value ≤ 0.01 was set to define statistically significant differences. The periods *1861–1901* and *1951–1971* show the highest number of statistically significant differences, suggesting more pronounced topological and hydraulic changes in the network during these transitions. This is likely related to the intense urban transformation and industrialization that took place in Turin starting in the 1950s.

To highlight temporal trends, Fig. 4 panel b illustrates the temporal evolution of the scale exponents, normalized to the values of the earliest historical phase (*before 1861*). The exponents h_1 and h_2, associated with network length, do not display a consistent trend over time, but both exhibit a pronounced negative peak in the *1861–1901* period. This may reflect reduced network tortuosity, possibly because this area served as a transitional expansion from the historic core, functioning as a connector between the older and more recently developed zones. The exponent p, associated with cross-sectional area, also shows a local minimum in the same period, followed by an increase in later decades. This suggests a progressively more conservative design approach (see Section 3.1.1), with larger conduit dimensions adopted in newer parts of the city to accommodate increasing runoff or uncertainty in rainfall projections. Another interesting aspect highlighted by panel Fig. 4b is the opposite trend of the coefficients in the two rainfall events considered. The exponent c_{1h} tends to increase over time, while c_{10min} decreases with the historical evolution of the network. This behaviour may be explained by the structural changes in the network over time: in more recent areas, drainage conduits are generally longer and connected to larger catchment areas (see Table 1), resulting in longer times of concentration. As a consequence, short-duration rainfall events (e.g., 10 min) are less effective in simultaneously activating the entire drainage network and tend to produce lower peak discharges, which is reflected in the decreasing values of c_{10min} with historical evolution. On the other hand, long-duration events (e.g., 1 h) ensure that even in more recent periods, where catchment areas are larger and conduits more extended and rectilinear, runoff can reach the outlet in a way that allows the entire basin to respond more or less simultaneously, effectively mobilizing the full network. As a result, unlike short-duration events, the scaling exponent c_{1h} does not decrease with the historical evolution of the network; rather, it tends to increase. This observed increase over time can be attributed to the expansion of impervious surfaces, which increases runoff generation for a given drained area, and to a network structure composed of longer, more rectilinear conduits. Such conduits provide more direct flow paths, allowing runoff from distant sub-catchments to reach the outlet nearly simultaneously during long-duration events, resulting in higher peak discharges and, consequently, a larger scaling exponent. Finally, regarding the exponent p of the S–A relationship, a clear increase can be observed during the third and fourth phases of the city's urban expansion (i.e., approximately the last century). This reflects a growing engineering awareness of the importance of increasing the conduit cross-sections along the network to cope with the corresponding downstream increase in discharge, thereby reducing the risk of hydraulic criticalities.

3.1.3. Comparison with river networks

Table 2 compares the scaling exponents observed in the Turin UDN with those typically found in natural river basins. These values are also shown in Fig. 3, where linear scaling trends are plotted for the UDN, and a small triangle indicates the exponent corresponding to rivers (see the legend and the *Rivers* slope marked inside the panels).

Regarding the length–area relationships (Eqs. (1) and (2)), the exponent h_1, which relates the length of the main conduit to the drained area, is closer with respect to h_2 to the values commonly observed in river systems. This reflects the methodological similarity: in both cases, the main channel length is used as the primary descriptor of drainage extent. By contrast, the exponent h_2, which accounts for the cumulative length of all secondary branches, is generally higher. This captures the more articulated structure of urban networks, where the layout is shaped by the built environment (e.g., roads, buildings), leading to a higher density of conduits compared to the simpler, tree-like topology of natural river basins. Unlike natural channels that evolve to minimize energy expenditure through path adjustment in deformable landscapes, urban conduits are constrained by the rigid 2D layout of the street network. The higher scaling exponents observed here suggest that the urban form imposes a degree of path redundancy and elongation that is structurally different from the self-organized optimality of natural basins. In general, both h_1 and h_2 values exceed the typical exponent observed in natural basins ($h \approx 0.6$), suggesting that network length, whether defined as L_{Hack} or L_{tot}, increases more rapidly with drained area in urban systems. This further supports the interpretation of urban networks as denser and more reticulated, with more complex hydraulic paths than their natural counterparts, revealing a "space-filling" strategy where every urban parcel must be directly connected to the drainage hierarchy.

Considering the power-law relationship between maximum discharge and drained area (Eq. (3)), the exponent c obtained for the 1-hour event approaches the typical value observed in natural river basins ($c \approx 0.75$). It is important to note that in fluvial studies, peak discharge is generally measured for extreme or long-duration rainfall events, ensuring that the entire basin contributes to the flow. In contrast, our analysis refers to fixed-duration events, and shorter durations (e.g., 10 min) may not activate the full network, resulting in lower exponents. Therefore, the lower values of c observed in urban drainage networks for short events do not necessarily indicate greater attenuation compared to natural basins, but rather reflect the limited spatial activation of the system under shorter forcing. The similarity with river basins emerges only for longer durations, when the hydrological response becomes more fully developed across the network.

Recent studies on natural fluvial networks have also highlighted the dynamic nature of the effective contributing area, which may expand or contract depending on event magnitude and runoff conditions (Barefoot et al., 2019; Costabile et al., 2024). While the present study does not explicitly investigate this aspect, focusing instead on two representative rainfall durations and a single return period, these works suggest that rainfall intensity and event magnitude may play an important role in shaping scaling relationships in drainage systems.

3.2. Centrality measures

After analysing the large-scale scaling relationships that describe how network geometry and hydraulics vary with drainage area, now the focus is on the internal organization of the Turin UDN. While the scaling laws highlighted global patterns of self-similarity and hydraulic efficiency across spatial scales, centrality metrics allow us to explore how these properties emerge locally through the network's connectivity structure. In other words, we move from the macroscopic behaviour captured by the scaling exponents to the microscopic topological organization that supports it. To this end, network centrality measures are examined, which quantify the relative importance of nodes in terms of their hydraulic connectivity and flow conveyance potential.

3.2.1. Betweenness centrality

The analysis of betweenness centrality (B) reveals the dominant influence of network topology over the choice of weighting schemes.

To evaluate the effect of weighting schemes on B, first B is calculated for each node in the unweighted network and for networks with different weights (see Section 2.5 for the definition of weights). For each configuration, nodes were ranked according to their centrality values.

The rankings between the unweighted and weighted cases are then compared in two ways (see rows in Table 3): first, considering all nodes, and second, focusing only on the top 90 nodes of the unweighted ranking to see how they were positioned in the weighted rankings. To quantify the consistency of the rankings, Spearman's correlation coefficient is calculated between weighted and unweighted cases. Values of Spearman coefficient close to 1 indicate very similar rankings, values close to 0 indicate the absence of a consistent relationship, and negative values indicate an inverse ranking. The results in Table 3 show that the ranking of nodes with the highest betweenness centrality remains largely unchanged when comparing each weighted configuration with the unweighted reference and between the two rainfall events considered.

Furthermore, focusing specifically on the composition of the most central nodes, the top 90 nodes of each weighted scheme largely coincide with those of the unweighted case, sharing at least 70% of the nodes in common. This analysis complements the ranking-based assessment, providing information on the stability of the most central nodes even if their exact order varies slightly.

The dominant role of the topology reflects the intrinsic properties of B, which depends on the number of shortest paths passing through a node. In highly hierarchical networks such as UDNs, shortest paths are often unique and largely determined by topology. Therefore, changing the edge weights (e.g., by length, diameter, or travel time) rarely alters which paths are selected, and the resulting B values remain stable. As will be shown in the next section, this contrasts with closeness centrality, which explicitly depends on the lengths of the shortest paths and is therefore more sensitive to the choice of weights.

Table 3
Spearman correlation coefficients comparing the values of weighted and non-weighted betweenness centrality B and closeness centrality C. For both B and C, the non-weighted centrality is computed once and used as a fixed reference in all pairwise comparisons. The correlation was investigated on all nodes and on the first 90 nodes with the highest unweighted values of B and C, respectively.

Betweenness centrality									
Nodes	B_L	$B_Q^{10\,min}$	$B_Q^{1\,h}$	$B_{Q^{-1}}^{10\,min}$	$B_{Q^{-1}}^{1\,h}$	$B_{Q/S}^{10\,min}$	$B_{Q/S}^{1\,h}$	$B_{S/Q}^{10\,min}$	$B_{S/Q}^{1\,h}$
All	0.977	0.978	0.974	0.981	0.976	0.983	0.977	0.983	0.978
90	0.814	0.883	0.876	0.845	0.843	0.916	0.845	0.849	0.857
Closeness centrality									
Nodes	C_L	$C_Q^{10\,min}$	$C_Q^{1\,h}$	$C_{Q^{-1}}^{10\,min}$	$C_{Q^{-1}}^{1\,h}$	$C_{Q/S}^{10\,min}$	$C_{Q/S}^{1\,h}$	$C_{S/Q}^{10\,min}$	$C_{S/Q}^{1\,h}$
All	0.984	0.983	0.977	0.853	0.795	0.989	0.980	0.864	0.816
90	−0.156	−0.131	−0.248	0.075	0.204	0.063	−0.120	−0.109	0.101

Table 4
Main statistics of the unweighted B, calculated on all nodes in each historical urban area: mean, standard deviation, coefficient of variation, skewness and kurtosis coefficient. Both the actual values and, in brackets, those of the normalized statistics with respect to the oldest zone (*Before 1861*) are shown.

Period	Mean	CV	Sk	Ku
Before 1861	3.07e−04 *(1.00)*	2.13 *(1.00)*	4.20 *(1.00)*	23.98 *(1.00)*
1861–1901	1.24e−04 *(0.41)*	2.17 *(1.02)*	5.19 *(1.24)*	33.81 *(1.41)*
1901–1951	1.44e−04 *(0.47)*	2.83 *(1.33)*	5.07 *(1.21)*	32.57 *(1.36)*
1951–1971	8.62e−05 *(0.28)*	1.90 *(0.89)*	3.56 *(0.85)*	17.35 *(0.72)*

Fig. 5 illustrates how the spatial distribution of the nodes with the highest B evolves as the city expands over time. Panel 5a shows the progressive evolution: each subpanel adds newer urban areas and highlights how high-centrality nodes emerge within them. In the complete network (final subpanel of Fig. 5a), high-B nodes cluster in the northern part of the city, particularly along three main east–west corridors (labelled 1–3 in the figure). The first corridor follows Corso Francia (1), while the other two (2–3) lie in the central UDN. Nodes in corridor 1 define the main structural backbone of the drainage system, namely key conduits responsible for conveying flows across large subcatchments. Corridors 2 and 3 reveal high-centrality nodes appearing at the interfaces between zones built in different periods, highlighting long-term structural continuity. Given their topological prominence, these areas are potential bottlenecks and thus critical for monitoring, maintenance, and inspection.

From a historical perspective, panel 5a reveals that even in the oldest part of the network (prior to 1861), part of the backbone (1) was already present along Corso Francia, supplemented by a secondary branch running parallel further south. With the expansion of the network, this primary structure was gradually reinforced. The more recent areas seem to integrate into this pre-existing skeleton, rather than introducing completely new central routes, especially visible in the development that took place between 1901 and 1951, where a continuation of the main backbone is evident.

Panel 5b offers an alternative reading by isolating each historical zone, showing the 20 most central nodes within each one independently. This helps identify secondary backbones that may not dominate at city scale but are locally significant. In the oldest area, the main backbone remains evident. During 1861–1901, a north–south extension becomes prominent. In 1901–1951, centrality consolidates along the historical spine, reinforcing its centripetal role in shaping the system. In contrast, in the most recent zone (1951–1971), high-B nodes are more spatially dispersed, suggesting a less hierarchical and more distributed network layout.

Fig. 5c illustrates the cumulative distribution of B. All zones show rapid initial growth and a plateau, confirming that most nodes have low centrality, with a few outliers dominating the network. The *before 1861* zone shows a less steep rise, indicating a broader group of moderately central nodes. This is related to the higher mean value of B, found in this zone. However, thereafter a softer plateau forms, suggesting that higher values are less frequent than in the other zones.

Finally, statistical metrics in Table 4 support qualitative findings, highlighting the persistence of a historical backbone and a gradual evolution towards a more distributed configuration. The average B are highest in the oldest part of the network (*Before 1861*), whereas more recent zones show lower means but higher coefficients of variation (CV), suggesting a greater heterogeneity that reduces dependence on a few critical nodes. Nevertheless, all zones show positive skewness and high kurtosis, indicating the persistence of a small number of dominant nodes.

3.2.2. Closeness centrality

The analysis of closeness centrality (C) follows the same approach adopted for betweenness centrality (B), comparing the rankings of nodes obtained under different weighting schemes with those from the unweighted network (see Table 3). In contrast to B, however, the introduction of weights has a much stronger effect on the results. When all nodes are considered, the Spearman correlation coefficients between weighted and unweighted cases remain relatively high (mostly above 0.8), indicating that the overall ranking of nodes is largely preserved across different weights. However, when the comparison is restricted to the 90 nodes with the highest unweighted C values, the correlation coefficients drop, reaching values close to zero or even negative. This suggests

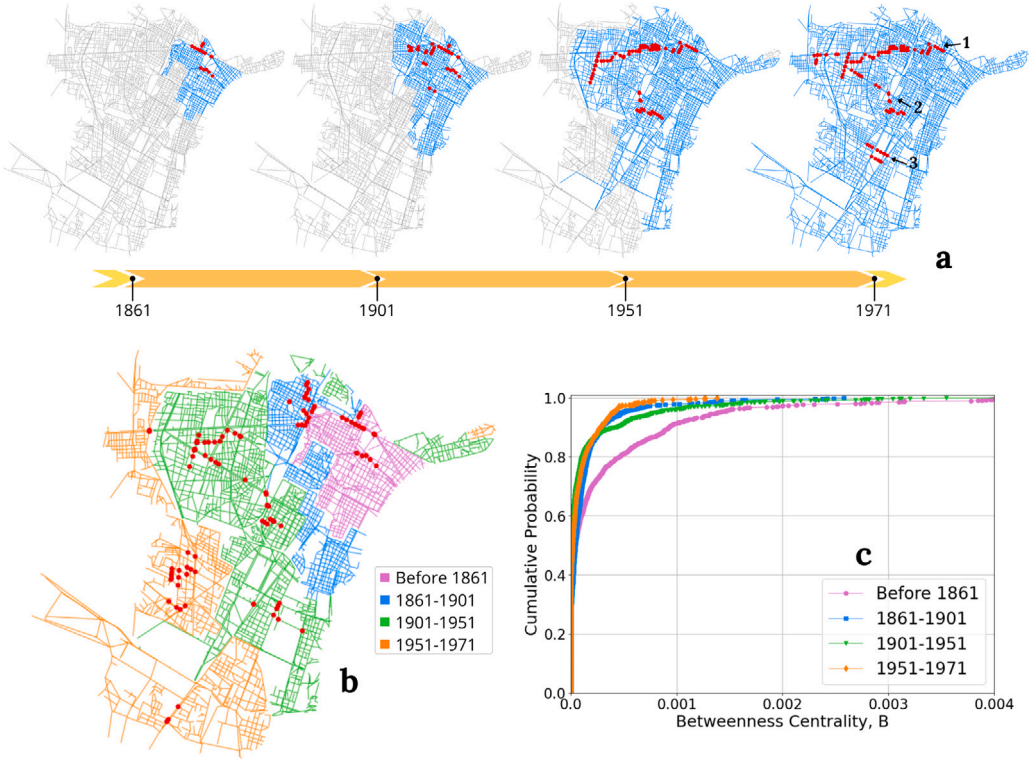


Fig. 5. Unweighted betweenness centrality B of the network divided into historical-urban zones. (a) Temporal evolution of the spatial distribution of nodes with high B, with progressive expansion of the network and selection of the 2% of nodes with the highest B relative to the total. (b) UDN graph in which historical subgraphs are considered separate and independent; in red, the 2% of nodes with the highest B value in each zone. (c) Cumulative density functions of B metrics, calculated by considering each zone as an independent subgraph.

Table 5
Spearman correlation coefficients comparing node rankings of weighted closeness centrality C between the two rain events, *10* min and *1* h. For each weighting scheme, the correlation was first investigated on *all* nodes and then on the first 90 nodes with the highest C value for the 10-minute event.

Nodes	C_Q	$C_{Q^{-1}}$	$C_{Q/S}$	$C_{S/Q}$
All	0.995	0.912	0.993	0.903
90	0.832	0.318	0.780	0.221

that, while the overall order of closeness values across the entire network remains consistent between weighted and unweighted cases, restricting to the most central nodes reveals a strong dependence on the chosen weight. Consistently, the overlap between the different sets of the 90 nodes with the highest closeness in the weighted and unweighted cases is less than 15% for all weights considered.

To further explore the sensitivity of closeness centrality (C) to the weighting scheme, the rankings obtained for the two rainfall events (10 min and 1 h) under each weight configuration (C_Q, $C_{Q^{-1}}$, $C_{Q/S}$, $C_{S/Q}$) were compared. As shown in Table 5, the Spearman correlation coefficients between the two events remain high when all nodes are considered (first row), indicating that event duration has a secondary influence compared with the choice of weighting scheme (see low correlation coefficients for closeness centrality in Table 3). It is then analysed how the ranking of the 90 nodes with the highest C values in the 10-minute event changes when considering their centrality for the 1 h event (second row in Table 5). In this case, the correlations decrease dramatically for weights $C_{Q^{-1}}$ and $C_{S/Q}$, revealing a marked dependence of the local centrality ranking on flow conditions. With such weights, the shortest paths favour conduits characterized by high flow rates. Thus, the low correlation indicates that high-flow areas are differently located for the two rain events.

For the following analyses, closeness is calculated using L as the edge weight. This choice is consistent with the definition of proximity as a measure of the distance of a node from all others in the network. In spatial networks such as UDNs, using pipe length provides the most direct and intuitive representation of distance, ensuring that shorter paths correspond to shorter geometries. Moreover, L is a purely geometric attribute that does not require any additional hydraulic simulations, making it a practical and

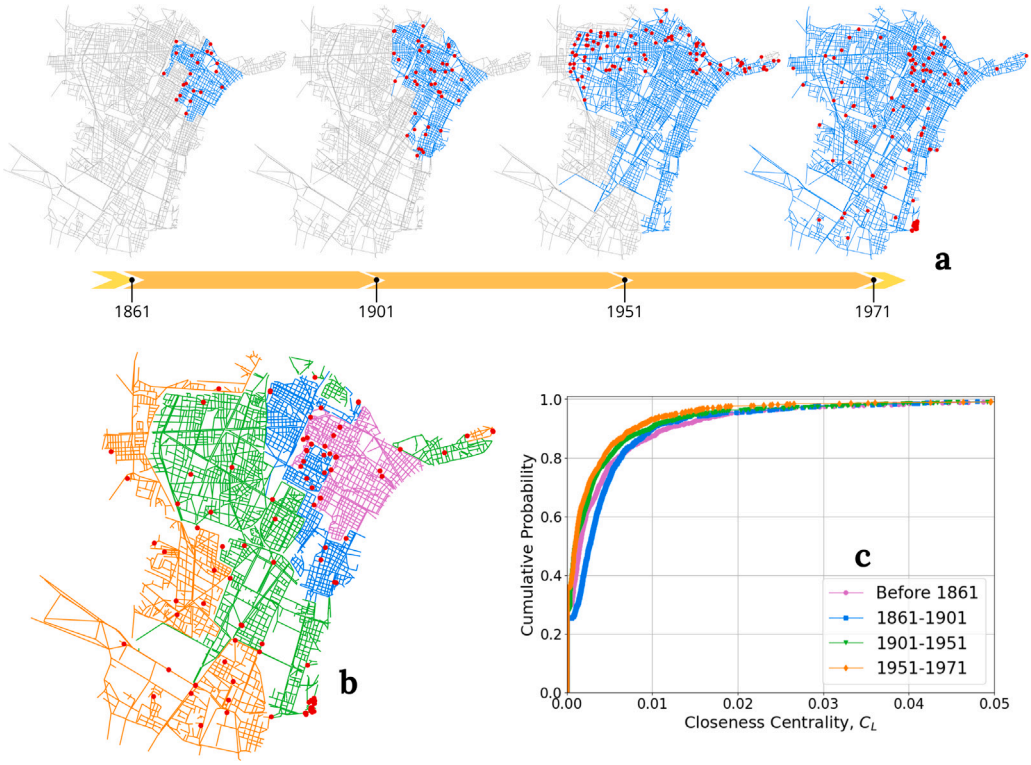


Fig. 6. Weighted closeness centrality C_L of the network divided into historical-urban zones. (a) Temporal evolution of the spatial distribution of nodes with high C_L, with progressive expansion of the network and selection of the 2% of nodes with the highest C_L relative to the total. (b) UDN graph in which historical subgraphs are considered separate and independent; in red, the 2% of nodes with the highest C_L value in each zone. (c) Cumulative density functions of C_L metrics, calculated by considering each zone as an independent subgraph.

robust choice for this analysis. Unlike flow-dependent weights, which can vary the spatial distribution of central nodes based on rainfall events, the L weight isolates the structural component of connectivity.

Fig. 6 is structured analogously to Fig. 5, but it focuses on the spatial distribution of nodes with the highest L-weighted closeness centrality (C_L) and on the cumulative evolution of this metric. In panel 6a—in contrast to the patterns observed for betweenness, where high-B nodes progressively define a clear backbone through time—high-C_L nodes appear more spatially scattered across the network. The temporal continuity visible for B is not evident here: instead, a marked discontinuity emerges around the 1951 expansion phase, when the most central nodes concentrate in the northern portion of the network. Nodes located in this area tend to be far from the main outfalls (see Fig. 1b) and they are reachable by many nodes through short average paths, which explains their high C_L values. However, this pattern does not persist when the full network is considered, where high-C_L nodes appear more dispersed across multiple clusters.

Panel 6b, which isolates each historical zone independently, reveals an interesting correspondence with the final cumulative map in panel 6a: several high-C_L nodes occur in similar locations despite the different spatial scopes of the two representations. This suggests that certain portions of the network consistently retain a locally central role even when analysed in different ways.

Finally, panel 6c shows the cumulative distributions of C_L, all exhibiting a rapid initial rise followed by a plateau, consistent with a large proportion of nodes having low centrality and therefore accessibility by others. The curves are broadly aligned across historical periods, with a slightly steeper increase for the 1861–1901 phase, hinting at a more compact and spatially efficient configuration during that stage of urban development.

Taken together, these results reinforce the contrast between the two centrality metrics: while betweenness highlights the hierarchical backbones that control long-range conveyance, closeness captures the local compactness and accessibility of the network, which appear to change consistently with urban growth.

3.2.3. Correlation between closeness centrality and hydraulic behaviour

Understanding whether the structural properties of the network influence its hydraulic response is a key aspect of this study. To explore this relationship, the existence of a power-law dependence between the closeness centrality weighted by length (C_L) and the maximum discharge (Q) observed during two rainfall events (Fig. 7) was tested:

$$Q \propto C_L^{\alpha}. \tag{7}$$

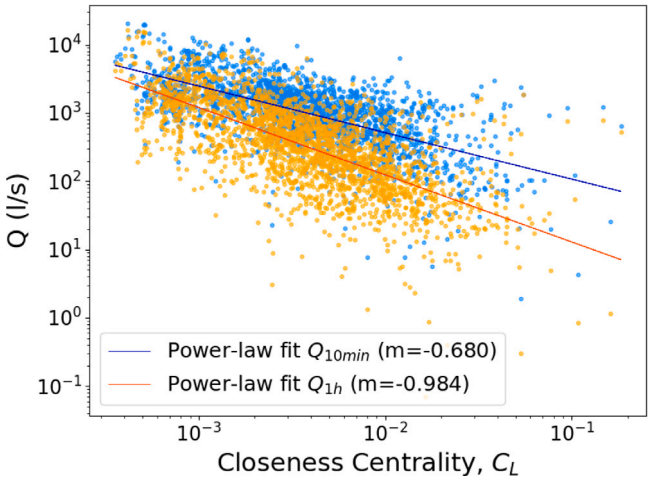


Fig. 7. Power law relationship applied to the entire UDN of Turin between the maximum discharge during the two rain events and the weighted closeness centrality C_L calculated at the various nodes. The scatter plot is shown in log–log scale and fitted by linear regression.

A statistically significant negative correlation was found between C_L and Q. The Pearson correlation coefficients were $\rho = -0.646$ for the 10-minute event and $\rho = -0.689$ for the 1-hour event (p-values < 0.001), indicating a moderate yet consistent relationship for both the events. The corresponding log–log regressions yielded exponents $\alpha = -0.680$ and $\alpha = -0.984$, respectively, both significant according to the t-test with p-value lower than 0.01.

The negative sign of α has a clear hydraulic interpretation that follows directly from the definition of closeness centrality. Since C_L is the inverse of the sum of the shortest-path distances to all other nodes, a higher C_L indicates that a node is, on average, topologically closer to the rest of the network (see Eq. (6)). In physical terms, these nodes occupy upstream or interior positions characterized by short drainage paths and small contributing areas, and therefore experience lower peak discharges. Conversely, nodes with low C_L have large total distances to other nodes, reflecting downstream locations that collect flow from many upstream elements. The longer flow paths and larger contributing areas associated with these distal positions naturally lead to higher Q values. Hence, the inverse relationship between Q and C_L expresses how the geometric proximity encoded in network topology mirrors the progressive hydraulic accumulation along the drainage system.

A comparison of the two rainfall events further revealed a statistically significant difference between their regression slopes ($p_v < 0.01$), suggesting that while the structural–hydraulic relationship is robust, the strength of this dependence may vary with event duration and associated flow dynamics.

4. Conclusions

In this work, an in-depth analysis of the urban drainage network of the city of Turin was carried out with the aim of exploring its structure and behaviour from both a topological and hydraulic perspective. Two complementary approaches were adopted and applied to the same system: (i) the analysis of scaling laws, traditionally used for natural river networks, to characterize the geometric and hydraulic self-organization of the UDN; and (ii) the use of centrality metrics, derived from CNT, to quantify the role and importance of individual nodes in the network's topology and flow transmission. Both approaches were examined in a temporal framework, by dividing the network into historical construction phases, and in a hydraulic framework, through the analysis of simulated maximum discharges for two rainfall events of different durations.

The main findings of the analysis, along with their potential implications, are summarized below:

1. Three scaling relationships were identified in the Turin UDN, relating the drained area to channel length, cross-section, and discharge. They all followed clear power-law behaviours, confirming the presence of hierarchical and self-similar structures qualitatively analogous to those observed in natural basins. The length–area relationship (Hack's law) showed exponents around 0.9, much higher than the ≈ 0.6 typical of rivers. This reflects the structural characteristics of UDNs, whose layout is constrained by the street system and therefore follows a space-filling logic, resulting in denser and more tortuous conduit paths. The section–area relationship shows a weak scaling ($p \approx 0.2$), indicating that conduit cross-sections increase with the drained area, although more slowly than discharge. This behaviour suggests that the increase in conduit capacity does not keep pace with the increase in discharge across the network. Finally, the discharge–area scaling ($Q \propto A^c$) shows that the scaling behaviour also extends to the hydraulic response of the network, linking the geometric structure of the system to its flow dynamics under rainfall forcing.

2. The discharge–area scaling ($Q \propto A^c$) showed a clear dependence on rainfall duration. The exponent c increased from about 0.5 for 10-minute storms to about 0.7 for 1-hour storms, reflecting the progressive activation of larger portions of the network: short events mainly mobilize local areas whereas longer events engage the system more completely, yielding higher c values closer to those observed in natural basins. A possible future development concerns a more systematic and dynamic analysis of the role of rainfall intensity. This aspect was not explored in depth in the present study, as only two rainfall durations and a single return period were considered. A more dynamic investigation could also allow for a more direct comparison with studies on natural river networks, which have shown that the contributing area can vary depending on the magnitude of the event and the runoff conditions.
3. The historical subdivision of the network revealed how structural changes influence hydraulic response. The most pronounced differences occurred between the *1861–1901* and *1951–1971* phases, corresponding to the city's post-war expansion. Newer areas have longer conduits draining larger subcatchments. Consequently, short-duration events activate only part of these expanded zones, whereas long-duration events allow nearly full network activation, contributing to the observed increase of c_{1h} over historical periods. This illustrates how urban growth and network extension modulate flow dynamics depending on rainfall duration.
4. Betweenness centrality (B) highlighted a stable backbone of the network: the highest-B nodes, which correspond to conduits conveying flow between large subcatchments, are largely unaffected by weighting schemes or rainfall events. This indicates that B primarily reflects the network's hierarchical topology rather than hydraulic variability. Spatially, these nodes cluster along a few dominant east–west corridors, forming the main "structural backbone" of the drainage system. While the network expanded over time, this backbone remained largely consistent, with new areas integrating into the pre-existing core rather than displacing it.
5. Closeness centrality (C_L) reveals nodes that are topologically "central", i.e., those with shorter average distances to all other nodes in the network. Unlike betweenness, the spatial distribution of high-C_L nodes is sensitive to the choice of edge weighting, reflecting how the definition of shortest paths affects perceived centrality. Spatially, high-C_L nodes are more scattered than the betweenness backbone, appearing throughout the network rather than along dominant corridors. This indicates that closeness captures local accessibility rather than global flow mediation, complementing the hierarchical backbone identified by betweenness.
6. A significant correlation emerged between L-weighted closeness centrality and maximum discharge, expressed through a scaling law, suggesting a potential predictive value of this purely topological metric with respect to a hydraulic quantity. Further studies, for example by analysing other UDNs or through hydraulic simulations under varying scenarios, could contribute to the generalization of this finding.

When considered together, the scaling and centrality analyses provide a coherent picture of the Turin UDN. The scaling laws confirm its hierarchical and self-similar organization, reflecting how geometric and hydraulic properties scale with drained area and evolve over time. Centrality metrics complement this view by revealing the role of individual nodes: betweenness identifies stable backbones that dominate flow conveyance, while closeness highlights locally central nodes whose structural positions correlate with peak discharges. The combination of these approaches shows that the network's topology and hydraulic response are closely intertwined, with historical backbones maintaining functional dominance even as the system expands, and newer zones integrating into the existing structure in a way consistent with the observed scaling laws.

Beyond the specific case study, these results suggest that urban drainage networks may share common structural and functional properties across different cities, similarly to what has been widely observed for natural river basins. The proposed combined framework, integrating scaling analysis and complex network metrics, therefore represents a promising approach for investigating the organization and functioning of urban drainage systems in different cities. Such an approach may support the identification of critical structural elements of drainage networks and contribute to their assessment, planning, and adaptation in the context of increasing urbanization and more frequent extreme rainfall events.

CRediT authorship contribution statement

Anna Eberrini: Writing – review & editing, Writing – original draft, Visualization, Methodology, Investigation, Formal analysis, Data curation. **Luca Ridolfi:** Writing – review & editing, Supervision, Methodology, Investigation, Conceptualization. **Sofia Fellini:** Writing – review & editing, Writing – original draft, Supervision, Methodology, Investigation, Conceptualization.

Declaration of competing interest

The authors declare that they have no known competing financial interests or personal relationships that could have appeared to influence the work reported in this paper.

Acknowledgements

The authors gratefully thank SMAT, the Turin water utility, for sharing the data of the Turin drainage network. We also express our gratitude to Francesco Loddo for sharing the results of the hydraulic model developed during his research and for his support in their interpretation.

Appendix A. Supplementary data

Supplementary material related to this article can be found online at https://doi.org/10.1016/j.ejrh.2026.103442.

Data availability

The preprocessed datasets and code underlying the analyses presented in this study are openly available on Zenodo at: https://doi.org/10.5281/zenodo.17702204.

References

Achour, M., Chahinian, N., Chancibault, K., Andrieu, H., Moussa, R., 2023. Morphometric properties, scaling laws and hydrologic response of the Greater Paris combined sewer system. Hydrol. Process. 37, e14984. http://dx.doi.org/10.1002/hyp.14984.

ARPA Piemonte, 2013. Heavy rainfall atlas of Piedmont (in Italian). URL https://www.arpa.piemonte.it/dato/atlante-piogge-intense. (Accessed November 2025).

Barefoot, E., Pavelsky, T.M., Allen, G.H., Zimmer, M.A., McGlynn, B.L., 2019. Temporally variable stream width and surface area distributions in a headwater catchment. Water Resour. Res. 55, 7166–7181. http://dx.doi.org/10.1029/2018WR023877.

Barthélemy, M., 2011. Spatial networks. Phys. Rep. 499, 1–101. http://dx.doi.org/10.1016/j.physrep.2010.11.002.

Barthelemy, M., 2022. Spatial networks. A Complete Introduction: From Graph Theory and Statistical Physics to Real-World Applications. Springer.

Biasin, A., Masiero, M., Amato, G., Pettenella, D., 2023. Nature-based solutions modeling and cost-benefit analysis to face climate change risks in an urban area: The case of turin (italy). Land 12, 280. http://dx.doi.org/10.3390/land12020280.

Brandes, U., 2001. A faster algorithm for betweenness centrality. J. Math. Sociol. 25, 163–177. http://dx.doi.org/10.1080/0022250X.2001.9990249.

Butler, D., Digman, C., Makropoulos, C., Davies, J.W., 2018. Urban Drainage. Crc Press.

Costabile, P., Costanzo, C., Lombardo, M., Shavers, E., Stanislawski, L.V., 2024. Unravelling spatial heterogeneity of inundation pattern domains for 2d analysis of fluvial landscapes and drainage networks. J. Hydrol. 632, 130728. http://dx.doi.org/10.1016/j.jhydrol.2024.130728.

Cremonini, R., Tiranti, D., Burzio, E., Brussolo, E., 2024. Studying intense convective rainfall in turin's urban area for urban flooding early warning system implementation. GeoHazards 5, 799–815. http://dx.doi.org/10.3390/geohazards5030040.

Crucitti, P., Latora, V., Porta, S., 2006. Centrality measures in spatial networks of urban streets. Phys. Rev. E 73, 036125. http://dx.doi.org/10.1103/PhysRevE.73.036125.

DPCM, 1996. Provisions relating to water resources (in Italian). Decree of the President of the Council of Ministers (DPCM), 4 March 1996. Government of Italy.

Estrada, E., 2012. The Structure of Complex Networks: Theory and Applications. American Chemical Society.

Falco, L., Morbelli, G., 1976. Turin, a Century of Urban Development: Notes for Reading a Capital City (in Italian). Celid Press.

Fellini, S., Salizzoni, P., Ridolfi, L., 2020. Centrality metric for the vulnerability of urban networks to toxic releases. Phys. Rev. E 101, 032312. http://dx.doi.org/10.1103/PhysRevE.101.032312.

Fellini, S., Salizzoni, P., Ridolfi, L., 2021. Vulnerability of cities to toxic airborne releases is written in their topology. Sci. Rep. 11, 23029. http://dx.doi.org/10.1038/s41598-021-02403-y.

Freeman, L., 1977. A set of measures of centrality based on betweenness. Sociometry 35–41. http://dx.doi.org/10.2307/3033543.

Giustolisi, O., Ridolfi, L., Simone, A., 2020. Embedding the intrinsic relevance of vertices in network analysis: the case of centrality metrics. Sci. Rep. 10, 3297. http://dx.doi.org/10.1038/s41598-020-60151-x.

Hack, J.T., 1957. Studies of Longitudinal Stream Profiles in Virginia and Maryland, vol. 294, US Government Printing Office.

Horton, R.E., 1945. Erosional development of streams and their drainage basins; hydrophysical approach to quantitative morphology. Geol. Soc. Am. Bull. 56, 275–370. http://dx.doi.org/10.1130/0016-7606(1945)56[275:EDOSAT]2.0.CO;2.

Ji, Y., Zheng, F., Yang, Y., Shuai, J., Huang, Y., Kapelan, Z., Savic, D., 2025. A comprehensive framework for evaluation of skeletonization impacts on urban drainage network model simulations. Water Resour. Res. 61, e2024WR038394. http://dx.doi.org/10.1029/2024WR038394.

Kitsak, M., Gallos, L.K., Havlin, S., Liljeros, F., Muchnik, L., Stanley, H.E., Makse, H.A., 2010. Identification of influential spreaders in complex networks. Nat. Phys. 6, 888–893. http://dx.doi.org/10.1038/nphys1746.

Kourtis, I.M., Tsihrintzis, V.A., 2021. Adaptation of urban drainage networks to climate change: A review. Sci. Total Environ. 771, 145431. http://dx.doi.org/10.1016/j.scitotenv.2021.145431.

Krueger, E., Klinkhamer, C., Urich, C., Zhan, X., Rao, P.S.C., 2017. Generic patterns in the evolution of urban water networks: Evidence from a large Asian city. Phys. Rev. E 95, 032312. http://dx.doi.org/10.1103/PhysRevE.95.032312.

Langhaar, H.L., 1962. Dimensional analysis and theory of models. New York, Wiley.

Leopold, L.B., Maddock, T., 1953. The Hydraulic Geometry of Stream Channels and Some Physiographic Implications, vol. 252, US Government Printing Office.

Leopold, L.B., Wolman, M.G., Miller, J.P., Wohl, E.E., 2020. Fluvial Processes in Geomorphology. Courier Dover Publications.

Li, Y., Wang, P., Lou, Y., Chen, C., Shen, C., Hu, T., 2024. Assessing urban drainage pressure and impacts of future climate change based on shared socioeconomic pathways. J. Hydrol.: Reg. Stud. 53, 101760. http://dx.doi.org/10.1016/j.ejrh.2024.101760.

Marsili, V., Alvisi, S., Maietta, F., Capponi, C., Meniconi, S., Brunone, B., Franchini, M., 2023. Extending the application of connectivity metrics for characterizing the dynamic behavior of water distribution networks. Water Resour. Res. 59, e2023WR035031. http://dx.doi.org/10.1029/2023WR035031.

Miller, J.D., Hutchins, M., 2017. The impacts of urbanisation and climate change on urban flooding and urban water quality: A review of the evidence concerning the united kingdom. J. Hydrol.: Reg. Stud. 12, 345–362. http://dx.doi.org/10.1016/j.ejrh.2017.06.006.

Montgomery, D.C., Peck, E.A., Vining, G.G., 2021. Introduction to Linear Regression Analysis. John Wiley & Sons.

Newman, M., 2018. Networks. Oxford University Press.

Phillips, J.D., Schwanghart, W., Heckmann, T., 2015. Graph theory in the geosciences. Earth-Sci. Rev. 143, 147–160. http://dx.doi.org/10.1016/j.earscirev.2015.02.002.

Ridolfi, L., Loddo, F., Boano, F., Raviola, F., Vesipa, R., 2023. Hydraulic Modelling of the Urban Drainage Network of Turin (in Italian). SMAT Report, Unpublished results.

Rigon, R., Rodriguez-Iturbe, I., Maritan, A., Giacometti, A., Tarboton, D.G., Rinaldo, A., 1996. On Hack's law. Water Resour. Res. 32, 3367–3374. http://dx.doi.org/10.1029/96WR02397.

Rinaldo, A., Banavar, J.R., Maritan, A., 2006. Trees, networks, and hydrology. Water Resour. Res. 42, http://dx.doi.org/10.1029/2005WR004108.

Rodrigues, F., 2018. Network centrality: An introduction. http://dx.doi.org/10.1007/978-3-319-78512-7_10.

Rodriguez-Iturbe, I., Marani, M., Rigon, R., Rinaldo, A., 1994. Self-organized river basin landscapes: Fractal and multifractal characteristics. Water Resour. Res. 30, 3531–3539. http://dx.doi.org/10.1029/94WR01493.

Rodriguez-Iturbe, I., Rinaldo, A., 1997. Fractal River Basins: Chance and Self-Organization. Cambridge University Press.

Rossman, L.A., Simon, M.A., 2022. Storm Water Management Model User's Manual Version 5.2. U.S. Environmental Protection Agency, Washington, D.C., URL https://www.epa.gov/system/files/documents/2022-04/swmm-users-manual-version-5.2.pdf, ePA/600/R-22/035.

Salata, S., Ronchi, S., Giaimo, C., Arcidiacono, A., Pantaloni, G.G., 2021. Performance-based planning to reduce flooding vulnerability insights from the case of turin (north-west italy). Sustainability 13, 5697. http://dx.doi.org/10.3390/su13105697.

Sarker, S., Veremyev, A., Boginski, V., Singh, A., 2019. Critical nodes in river networks. Sci. Rep. 9, 11178. http://dx.doi.org/10.1038/s41598-019-47292-4.

Sassolas-Serrayet, T., Cattin, R., Ferry, M., 2018. The shape of watersheds. Nat. Commun. 9, 3791. http://dx.doi.org/10.1038/s41467-018-06210-4.

Saxena, A., Iyengar, S., 2020. Centrality measures in complex networks: A survey. http://dx.doi.org/10.48550/arXiv.2011.07190, ArXiv.

Scarsoglio, S., Laio, F., Ridolfi, L., 2013. Climate dynamics: a network-based approach for the analysis of global precipitation. PLoS One 8, e71129.

Simone, A., Cesaro, A., Del Giudice, G., Di Cristo, C., Fecarotta, O., 2022. Potentialities of complex network theory tools for urban drainage networks analysis. Water Resour. Res. 58, e2022WR032277. http://dx.doi.org/10.1029/2022WR032277.

Simone, A., Ridolfi, L., Berardi, L., Laucelli, D., Giustolisi, O., et al., 2018. Complex network theory for water distribution networks analysis. EPiC Ser. Eng. 3, 1971–1978.

Suweis, S., Konar, M., Dalin, C., Hanasaki, N., Rinaldo, A., Rodriguez-Iturbe, I., 2011. Structure and controls of the global virtual water trade network. Geophys. Res. Lett. 38, http://dx.doi.org/10.1029/2011GL046837.

Tarboton, D.G., Bras, R.L., Rodriguez-Iturbe, I., 1991. On the extraction of channel networks from digital elevation data. Hydrol. Process. 5, 81–100. http://dx.doi.org/10.1002/hyp.3360050107.

Vesipa, R., Ridolfi, L., Fellini, S., 2026. Revealing the topological drivers of hydraulic transients in water distribution networks. Water Resour. Res. 62, http://dx.doi.org/10.1029/2025WR040594.

Wasserman, S., Faust, K., 1994. Social Network Analysis: Methods and Applications. Cambridge University Press.

Yang, S., Paik, K., McGrath, G.S., Urich, C., Krueger, E., Kumar, P., Rao, P.S.C., 2017. Functional topology of evolving urban drainage networks. Water Resour. Res. 53, 8966–8979. http://dx.doi.org/10.1002/2017WR021555.

Yazdanfar, Z., Sharma, A., 2015. Urban drainage system planning and design–challenges with climate change and urbanization: a review. Water Sci. Technol. 72, 165–179. http://dx.doi.org/10.2166/wst.2015.207.

Yu, J., Chen, Y., Zhu, C., Di, Y., Li, Z., Fang, G., Liu, C., Zou, B., Lyu, H., 2024. Evaluation of water system connectivity based on node centrality in the Tarim River Basin, Xinjiang, China. Water 16, 3031. http://dx.doi.org/10.3390/w16213031.

Zhou, Q., 2014. A review of sustainable urban drainage systems considering the climate change and urbanization impacts. Water 6, 976–992. http://dx.doi.org/10.3390/w6040976.